

# Quasiparticle and Cooper Pair Tunneling in the Vortex State of $\text{Bi}_2\text{Sr}_2\text{CaCu}_2\text{O}_{8+\delta}$

N. Morozov<sup>1</sup>, L.N. Bulaevskii<sup>1</sup>, M.P. Maley<sup>1</sup>, Yu.I. Latyshev<sup>2†</sup>, and T. Yamashita<sup>2</sup>

<sup>1</sup>*Los Alamos National Laboratory, Los Alamos, NM 87545*

<sup>2</sup>*Research Institute of Electrical Communication, Tohoku University, 2-1-1, Katahira, Aoba-ku, Sendai 980-8577, Japan*  
(February 1, 2008)

From measurements of the  $c$ -axis I-V characteristics of intrinsic Josephson junctions in  $\text{Bi}_2\text{Sr}_2\text{CaCu}_2\text{O}_{8+\delta}$  (Bi-2212) mesas we obtain the field dependence ( $\mathbf{H} \parallel c$ ) of the quasiparticle (QP) conductivity,  $\sigma_q(H, T)$ , and of the Josephson critical current density,  $J_c(H, T)$ .  $\sigma_q(H)$  increases sharply with  $H$  and reaches a plateau at  $0.05 \text{ T} < H < 0.3 \text{ T}$ . We explain such behavior by the dual effect of supercurrents around vortices. First, they enhance the QP DOS, leading to an increase of  $\sigma_q$  with  $H$  at low  $H$  and, second, they enhance the scattering rate for specular tunneling as pancakes become disordered along the  $c$ -axis at higher  $H$ , leading to a plateau at moderate  $H$ .

PACS numbers: 74.25.Fy, 74.50.+r, 74.72.Hs

Important information regarding pairing symmetry in cuprate superconductors has been obtained from the quasiparticle (QP) spectrum. Strong evidence in favor of  $d$ -wave symmetry of the superconducting order parameter has come from ARPES and STM experiments [1,2]. The effect of a magnetic field on QP properties becomes particularly interesting because, in the nodal regions of a  $d$ -wave gap, it probes fine details of the low-energy QP spectrum and its alteration by supercurrents surrounding vortices. An increase of QP density of states (DOS) produced by the Doppler shift of near-nodal QP energies by the vortex supercurrents is predicted to lead to an increasing QP DOS with magnetic field [3,4]. This effect was apparently observed in calorimetric measurements in HTS [5]. In-plane thermal conductivity measurements however have indicated a more complex magnetic field dependence. At low temperatures  $\kappa_{ab}(H)$  was seen to increase sublinearly with field in agreement with predictions of the Volovik mechanism [8]. At higher temperatures,  $T > 2\text{--}5 \text{ K}$ ,  $\kappa_{ab}(H)$  was observed in Bi-2212 to first decrease with increasing magnetic field and then reach a plateau and remain constant up to fields of several tesla [6]. A similar behavior was observed also in YBCO [7]. Franz [9] attempted to explain the high temperature plateau behavior as resulting from a compensating effect of QP scattering from in-plane vortex disorder. While this provides a qualitative description of the high temperature behavior, it fails to account for the fact that the low temperature sublinear increase with  $H$  shows no effect of a compensating scattering from vortex disorder. Thus, the thermal measurements have presented an ambiguous picture of the competing contributions of vortices, increasing DOS and scattering, to QP transport.

More direct information on QP properties can be obtained by study of the charge transport, namely, the  $c$ -axis conductivity  $\sigma_c(H)$ , in Josephson-coupled layered HTS. Recent measurements on micron-sized mesas of Bi-2212 have demonstrated that QP conductivity in the superconducting state can be accessed by exceeding the Josephson critical current, switching the interlayer

Josephson junctions into the resistive state and returning to low currents on the resistive branch [10]. Recent theoretical development has shown that  $c$ -axis QP conductivity is determined by the QP DOS and the effective scattering rate for interlayer tunneling [11]. In this Letter we provide an unambiguous determination of the effects of vortices on the QP DOS and on the effective scattering rate for  $c$ -axis tunneling.

We study the effect of vortices on the  $c$ -axis QP conductivity,  $\sigma_q(H, T)$ , by measuring the I-V characteristics in the resistive state of small Bi-2212 mesas as a function of the magnetic field  $0 < H < 9 \text{ T}$  applied parallel to the  $c$ -axis. At the same fields we extract the dependence of the Josephson critical current density  $J_c(H, T)$  to obtain independent information on  $c$ -axis correlation of pancake vortices. Our main finding is that  $\sigma_q(H, T)$  first increases rapidly with field, then reaches a plateau at  $40 \text{ mT} < B < 0.5 \text{ T}$  due to the dual role of vortices. As the field further increases,  $\sigma_q(H)$  increases linearly, as was found previously [12]. We observe a moderate drop of  $J_c(H, T)$  with  $H$  in the field range of the plateau and then a faster drop of  $J_c$  in fields where the linear growth of  $\sigma_q(H)$  takes place. This drop indicates strong disorder in vortex positions along the  $c$ -axis in high fields in agreement with enhancement of the effective scattering rate at interlayer tunneling responsible for plateau formation.

For our experiments we used several step-like mesa samples with  $T_c = 73 \text{ K}$  and area  $S = 2 \times 2 \mu\text{m}^2$  manufactured from high-quality Bi-2212 whiskers utilizing the

TABLE I. Bi-2212 mesa samples;  $S \approx 4 \mu\text{m}^2$ ,  $T_c \approx 73 \text{ K}$ .  $R_n$  is the resistance at  $T = 300 \text{ K}$ ,  $N$  is the number of intrinsic junctions,  $J_c$  is the maximum critical current density ( $H = 0$ ),  $\gamma$  is the in-plane effective scattering rate, and  $\sigma_q(0, 0)$  is the QP conductivity at  $H = 0$ ,  $T \rightarrow 0$ .

mesa	$R_n, \text{k}\Omega$	$N$	$J_c @ 4 \text{ K}, \text{A/cm}^2$	$\gamma, \text{K}$	$\sigma_q(0, 0), (\text{k}\Omega \text{ cm})^{-1}$
m1	2.1	42	830	32.0	1.5
m2	4.5	90	500	31.8	2.1
m3	0.85	17	1100	34.0	4.3
m4	3.0	60	450	—	1.8

Focused Ion Beam technique [10]. In this Letter we present data obtained on 4 typical samples (See Table I). We performed measurements of I-V characteristics at different magnetic fields and temperatures in a standard He-flow cryostat, which provided temperature stabilization better than  $\pm 10$  mK. Magnetic fields up to 9 T were applied along the  $c$ -axis of the mesa by a superconducting solenoid. The intrinsic Josephson junctions in high quality mesas have a small shunting conductance due to QP tunneling and thus behave as underdamped junctions with highly hysteretic I-V dependence. Typical multibranching I-V curves in zero-field-cooled (ZFC) mode at  $T = 4$  K are shown in Fig. 1. The increasing current branch provides information on the critical current, whereas the decreasing current branch corresponds to the resistive state, where current is due to QP tunneling. Direct comparison of I-V curves at  $H = 0$  T, 0.05 T, and 0.15 T (Fig. 1) shows that a) critical currents drop with  $H$ , and thus all branches collapse to that of the resistive state, and b) variation of critical current for different junctions increases with  $H$  in comparison with that at  $H = 0$

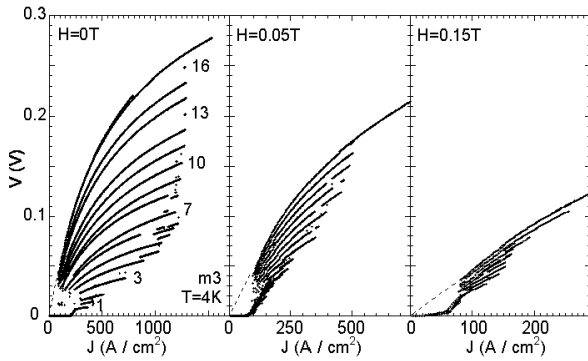


FIG. 1. I-V curves for Bi-2212 mesa m3 at  $H = 0$ ,  $H = 0.05$  T, and  $H = 0.15$  T. For this sample all 17 branches are resolved.

It is important that the branch of I-V curves for decreasing current, when all junctions are in the resistive state, is the same for all current sweeps for both field cooling (FC), and ZFC (Fig. 2). This observation allows us to study the field dependence of QP conductivity,  $\sigma_q(H, T)$ , measured in ZFC. The value of average QP resistivity,  $\langle \rho_q \rangle$ , was obtained from the all-junction resistive-state I-V curve at low currents as described in Ref. [10], and  $\sigma_q = 1/\langle \rho_q \rangle$  was calculated.

In contrast to the behavior of  $\sigma_q(H)$ , the distribution of critical current over junctions is different for FC and ZFC modes. The distribution of  $J_c(B, T)$  over junctions in small-area mesas arises because a) at  $T \rightarrow 0$  and  $H = 0$  junctions are inequivalent with respect to  $J_c$  at least due to their geometrical position in the mesa, b) at nonzero field  $J_c(B, 0)$  for a junction between layers  $n$  and  $n + 1$

depends on vortex positions in the layers, which vary randomly with  $n$  in the case of uncorrelated pinning [13], and c) at nonzero  $T$ , jumps from the superconducting

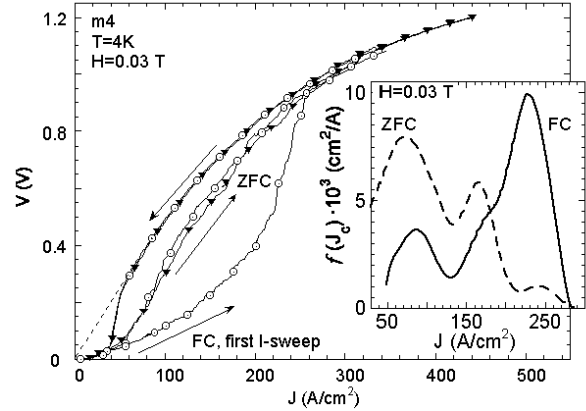


FIG. 2. I-V curves for  $H = 0.03$  T, FC ( $\circ$ ) and ZFC ( $\blacktriangledown$ ) modes. In the FC mode vortices initially are better correlated, providing larger  $J_c$ . Switching the junctions in the resistive state suppresses  $c$ -axis pancake correlations, and the system becomes similar for both FC and ZFC. Inset: the distribution of  $J_c$  in junctions for ZFC (dash) and FC (line) modes.

state to a resistive one occur at different  $J$  due to thermal fluctuations [14]. We can find the distribution function of the critical current density,  $f(J)$ , from our data as  $f(J) = d(V_{\uparrow}/V_{\downarrow})/dJ$ , where  $V_{\uparrow}(J)$  [ $V_{\downarrow}(J)$ ] are voltages on increasing [decreasing] currents. The inset in Fig 2 shows smoothed distribution functions  $f(J)$  for FC and ZFC modes. We note that average critical current density,  $\langle J_c(H = 0.03\text{T}) \rangle$ , obtained in the FC mode at 4 K is larger by the factor  $\approx 2$  than that in the ZFC mode. This result is in agreement with measurements [15] of the Josephson plasma resonance (JPR) frequency. Below the irreversibility line (in the vortex glass phase) the JPR

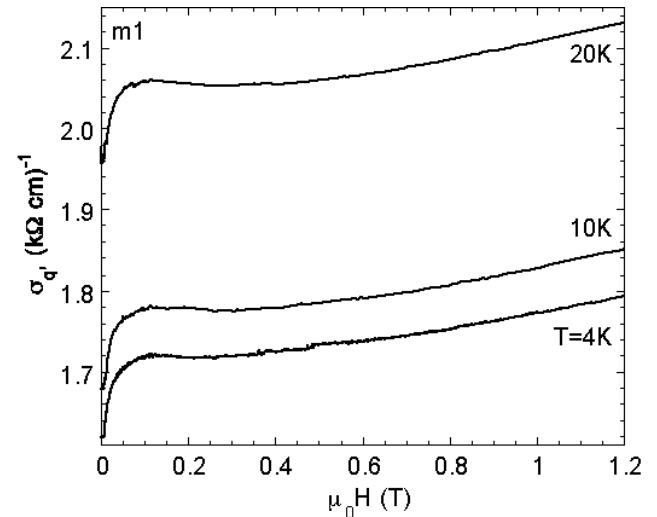


FIG. 3. For mesa m1  $\sigma_q(V \rightarrow 0)$  is plotted vs.  $H$  for three different temperatures.

frequency in the FC mode was found to be larger than in the ZFC mode. A very important new observation is that curves obtained in the second and subsequent current sweeps in the FC mode are similar, and they practically coincide with those observed in the ZFC mode. This shows that in our thin plate-like mesas suppression of Josephson coupling by switching into the resistive state *irreversibly* produces pancake disorder comparable to that produced by ramping the magnetic field, i.e. vortices do not change their positions when one goes from the resistive state back into the superconducting state.

In Fig. 3 we present our principal result showing a typical dependence of QP conductivity as a function of magnetic field. The conductivity rises steeply with magnetic field, reaches a distinct plateau, and then rises more gradually with field at higher fields. Below we explain our experimental data using theoretical results [11] for  $\sigma_q(B)$  and an estimate for  $J_c(B, T)$  in small mesas.

Let us outline the main theoretical predictions [11] for QP conductivity  $\sigma_q(B)$  in the mixed state. QP tunneling in a  $d$ -wave layered superconductor in the presence of vortices is determined by two competing mechanisms:  $\sigma_q$  is proportional to the QP DOS and inversely proportional to the effective scattering rate for interlayer tunneling,  $\gamma_c$ . In-plane supercurrents around vortices lead to a DOS increase near gap nodes proportional to the averaged Doppler shift in the QP spectrum,  $E_H \approx v_F(B/\Phi_0)^{1/2}$  at  $\gamma \ll E_H \ll \Delta_0$ , where  $\gamma$  is the impurity induced effective in-plane scattering rate and  $\Delta_0$  is the gap amplitude. In the framework of the specular tunneling model, when in-plane momentum is conserved at tunneling,  $\sigma_q$  will increase strongly with  $B$  due to DOS enhancement when vortices are correlated along the  $c$ -axis. If  $c$ -axis correlation of pancakes is absent, the effective scattering rate  $\gamma_c$  increases with  $B$  due to different Doppler shifts at equivalent points in adjacent layers, suppressing tunneling. There is a characteristic field,  $B_\gamma = \Phi_0 \gamma^2 / \hbar^2 v_F^2$ , estimated as  $B_\gamma \sim 0.2 - 0.6$  T, which corresponds roughly to the field at which the variation of Doppler shift becomes comparable to the scattering rate  $\gamma$ . The latter may be estimated from the temperature dependence  $\sigma_q(0, T) = \sigma_q(0, 0)(1 + cT^2)$ , where  $c = \pi^2/18\gamma^2$ . Values of  $\gamma$  for mesas studied are presented in the Table I. It was predicted that in the quasiclassical approach, valid at  $E_H \ll \Delta_0$ , when one accounts for Doppler shifts only, one gets  $\gamma_c \approx E_H$  in fields  $B \geq B_\gamma$ . In this field range increase in scattering caused by Doppler shift variation in adjacent layers compensates in  $\sigma_q(H)$  the increase in DOS, providing a nearly field independent  $\sigma_q(H)$ . Corrections to this approach lead to a weak linear increase of QP conductivity at  $B_\gamma \ll B \ll B_0$ ,

$$\sigma_q(B)/\sigma_q(0) = C_1 + B/B_0, \quad (1)$$

where  $B_0 \approx 20$  T. Here  $C_1$  depends on in-plane pancake ordering. The values of  $C_1$  between 1.07 and 1.22

were calculated for a 2D vortex liquid depending on the effective temperature of vortex disorder  $T_{eff}$  [11].

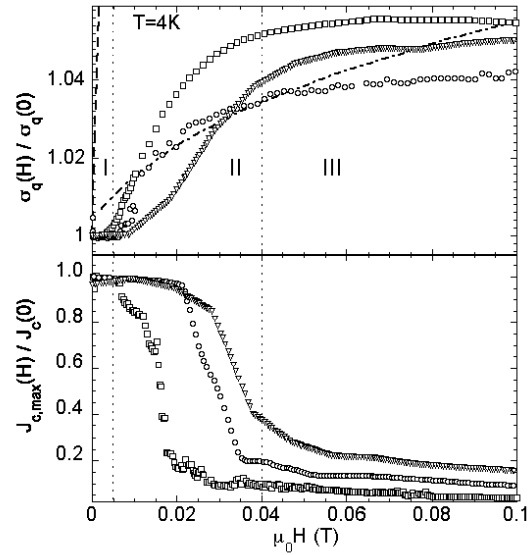


FIG. 4. For mesas [m1 ( $\square$ ), m2 ( $\circ$ ) and m3 ( $\nabla$ )] the normalized  $\sigma_q$  (top) and  $\langle J_c \rangle$  (bottom) are plotted vs.  $H$ . Three different regimes with respect to  $H$  are marked by vertical dotted lines. The theoretical curves of  $\sigma_q(B)$  for correlated (dashed) and  $c$ -axis-uncorrelated (dash-dotted) vortex systems are shown for  $B_\gamma = 0.6$  T,  $\Delta_0 = 25$  meV, and  $T_{eff} = 0.06$  ( $\Phi_0^2 s / 8\pi^2 \lambda_{ab}^2$ ) [11].

The field dependence of the Josephson critical current in the vortex glass state for  $\mathbf{H} \parallel c$  comes from the dependence of  $J_c(B, T) = J_c(0, T) \langle \cos \varphi_{n,n+1}(\mathbf{r}) \rangle$  on the gauge-invariant phase difference  $\varphi_{n,n+1}(\mathbf{r})$  induced by pancakes when they are misaligned in the layers  $n$  and  $n+1$  due to random pinning. Correlations of pancakes in neighboring layers, leading to lower energy, are induced by magnetic coupling of pancakes and by Josephson interlayer coupling; both tend to align vortices along the  $c$ -axis. Maximum  $J_c$  in the vortex glass phase may be achieved by adjustment of pancake positions to minimize both Josephson and pinning energy [16]. This effect is negligible for the ZFC mode and, as shown above, for the FC mode after switching from the resistive state where Josephson coupling is absent. For the critical current  $J_c(B, 0)$  in mesas with the size  $L \ll \lambda_J^2/a$ , the relations

$$\frac{\langle J_c^2(B, 0) \rangle}{J_c^2(0, 0)} = \int \frac{d\mathbf{r} d\mathbf{r}'}{L^4} \langle \exp[i\varphi_{n,n+1}(\mathbf{r}) - i\varphi_{n,n+1}(\mathbf{r}')] \rangle, \quad (2)$$

$$\varphi_{n,n+1}(\mathbf{r}) = \sum_i \phi_v(\mathbf{r} - \mathbf{r}_{ni}) - \phi_v(\mathbf{r} - \mathbf{r}_{n+1,i})$$

hold [13]. Here  $a = (\Phi_0/B)^{1/2}$  is the intervortex distance,  $\lambda_J$  is the Josephson length,  $\sim 1 \mu m$  in typical mesas,  $\phi_v(\mathbf{r})$  is the polar angle of the point  $\mathbf{r}$ , and  $\mathbf{r}_{ni}$  is the coordinate of pancake  $i$  in the layer  $n$ . In Eq. (2) the integrand,  $\langle \exp[i\varphi_{n,n+1}(\mathbf{r}) - i\varphi_{n,n+1}(\mathbf{r}')] \rangle$ , drops with  $|\mathbf{r} - \mathbf{r}'|$

on the scale  $a$  at  $a \ll L$ . Then we estimate  $\langle J_c(B, 0) \rangle < \langle J_c^2(B, 0) \rangle^{1/2} \approx J_c(0, 0)(\Phi_0/BL^2)^{1/2}$ . Thermal fluctuations cause jumps into the resistive state at  $J < J_c(B, 0)$  and diminish additionally the average critical current. When the Josephson energy,  $\Phi_0 \langle J_c(B, 0) \rangle L^2/2\pi c$ , becomes less than  $\approx 10T$  (see Eq. (6.18) in Ref. [14]), thermal fluctuations practically eliminate the superconducting part of I-V curves. For our mesas this occurs in fields  $\gtrsim 0.01$  T at  $T = 4$  K.

Now we explain our experimental results using these theoretical results. In Fig. 4 we plot the low-field part of the  $\sigma_q(H)$  dependence together with extracted  $J_{c,max}(H)$  for three different samples. Shown here are also theoretical curves calculated for  $\sigma_q(B)$  in the case of  $c$ -axis-correlated and uncorrelated vortex states [11], indicating clearly that  $c$ -axis disorder is responsible for strong suppression of  $\sigma_q$  at high fields. The experimentally observed  $\sigma_q(H)$  can be divided into three segments as magnetic field increases as shown in Fig. 4. These segments correspond to appropriate parts of the field dependence of the critical current density,  $J_{c,max}$ , obtained in the ZFC mode, presented in the lower part of Fig. 4. At very low fields,  $H \lesssim 5$  mT, (Segment I) there is practically no change in  $\sigma_q$  and in  $J_{c,max}$ . This regime corresponds to the Meissner state of the sample. Note that, despite the suppression of supercurrent along the  $c$ -axis by applied transport current in the resistive state, the in-plane Meissner currents persist, preventing pancake vortex entrance into the sample. Only when the magnetic field  $H$  exceeds  $\sim 5$  mT do pancakes enter into the sample. In the intermediate field range,  $5 \leq H < 40$  mT, (segment II) the experimental results for  $\sigma_q(H)$  lay slightly above the curve for uncorrelated vortices but well below the curve for the  $c$ -axis-correlated vortex state. This indicates that weak  $c$ -axis vortex correlations are present in this field range. Weakly correlated pancakes affect  $J_c$  much more strongly than  $\sigma_q$ , because increase in  $B$  leads to decrease of  $J_c$  (the fluctuations of the phase difference increase and  $\langle \cos \varphi_{n,n+1}(\mathbf{r}) \rangle$  drops), while for  $\sigma_q$  the increase of DOS is compensated partly by an increase of  $\gamma_c$ . As the field continues to increase above 40 mT (segment III) increase of  $\sigma_q$  with  $H$  is slowing down due to a stronger decrease of  $c$ -axis correlations and, respectively, stronger increase of  $\gamma_c$ . This leads to formation of the plateau (or even dip) in the range  $40 < H < 300$  mT.

This scenario is confirmed by the behavior of  $J_{c,max}(H)$ . A sharp drop in  $c$ -axis correlations above 40 mT was observed in Bi-2212 single crystals as the second peak effect. It was shown by neutron scattering [17] and JPR frequency study [18] that here the vortex system decomposes into a  $c$ -axis-uncorrelated vortex glass. Accordingly, the  $c$ -axis critical current density,  $J_{c,max}$ , drops rapidly, as seen clearly in the insert in Fig. 1. At fields above 0.5 T the dependence  $\sigma_q(H)$  changes again, switching to the linear growth, observed and discussed in our previous work [12]. We obtain  $B_0 \sim 20$  T and

$C_1 \sim 1.04$ . We see that  $C_1$  is smaller than that calculated for the vortex liquid, and this means that in-plane ordering in the vortex glass is better than in the liquid.

To conclude, we observed a plateau in  $\sigma_q(H)$ , which formed as a result of the compensation of the increase of QP DOS due to Volovik effect by the increase of the effective scattering rate for tunneling due to  $c$ -axis pancake disorder. The field dependence of the QP interlayer conductivity is sensitive to the structure of vortex state. We found that in the vortex glass adjustment of vortex positions to the Josephson interlayer coupling depends on the way this vortex state was achieved. Critical current in the FC mode is  $\sim 2$  times larger than that obtained in the ZFC mode or in the FC mode after switching from the resistive state. The  $d$ -wave pairing model in the clean limit with resonant intralayer scattering and significant contribution of specular interlayer tunneling provides an explanation for the  $c$ -axis electrical transport in the vortex state of Bi-2212 crystals at low temperatures and low magnetic fields.

We thank A.M. Nikitina for providing us with Bi-2212 single crystal whiskers, Ch. Helm, A.E. Koshelev, and I.B. Vekhter for useful discussions, and J.Y. Coulter for the technical assistance. This work was supported by the Los Alamos National Laboratory under the auspices of the U.S. Department of Energy, CREST, the Japan Science and Technology Corporation, and the Russian State Program on HTS under grant No. 99016.

---

<sup>†</sup> Permanent address: Institute of Radio Engineering and Electronics RAS, 11 Mokhovaya, 103907, Moscow.

- [1] H. Ding *et al.*, Phys. Rev. Lett. **74**, 2784 (1995); J. Mesot *et al.*, *ibid.* **83**, 840 (1999).
- [2] Y. DeWilde *et al.*, Phys. Rev. Lett. **80**, 153 (1998).
- [3] L.P. Gor'kov and P.A. Kalugin, JETP Lett. **41**, 253 (1985).
- [4] G.E. Volovik, JETP Lett. **58**, 6 (1993).
- [5] K.A. Moler *et al.*, Phys. Rev. Lett. **73**, 2744 (1994); J.W. Loram *et al.*, J. Phys. Chem. Sol. **59**, 2091 (1998).
- [6] K. Krishana *et al.*, Science **277**, 83 (1997); H. Aubin *et al.*, *ibid.* **280**, 9a (1998); Y. Ando *et al.*, cond-mat/9812265, 1999.
- [7] M. Chiao *et al.*, Phys. Rev. Lett. **82**, 2943 (1999).
- [8] H. Aubin *et al.*, Phys. Rev. Lett. **82**, 642 (1999).
- [9] M. Franz, Phys. Rev. Lett. **82**, 1760 (1999).
- [10] Yu.I. Latyshev *et al.*, Phys. Rev. Lett. **82**, 5345 (1999).
- [11] I. Vekhter *et al.*, Phys. Rev. Lett. **84**, 1296 (2000).
- [12] N. Morozov *et al.*, Phys. Rev. Lett. **84**, 1784 (2000).
- [13] M.V. Fistul, JETP Lett. **52**, 192 (1990).
- [14] M. Tinkham, *Introduction to Superconductivity*, (McGraw-Hill, 1996).
- [15] Yu. Matsuda, *et al.*, Phys. Rev. Lett. **78**, 1972 (1997).
- [16] A.E. Koshelev *et al.*, Phys. Rev. B **53**, 2786 (1996).
- [17] R. Cubitt and E.M. Forgan, Nature **365**, 407 (1993).
- [18] M.B. Gaifullin *et al.*, Phys. Rev. Lett. **84**, 2945 (2000).